NUCLEAR STRUCTURE OF THE MIRROR PAIR ^{25}Mg AND ^{25}Al WITHIN THE SHELL MODEL FRAMEWORK*

A. Selim, M. Bouhelal

Laboratory of Applied and Theoretical Physics (LATP)
Echahid Cheikh Larbi Tebessi University
Constantine Road, Tebessa, 12022, Algeria

F. Haas

IPHC, CNRS/IN2P3, Université de Strasbourg
67037 Strasbourg, Cedex2, France

Received 31 October 2025, accepted 2 February 2026, published online 31 March 2026

The mirror nuclei ^{25}Mg and ^{25}Al play a critical role in nucleosynthesis processes, as they participate in the slow neutron capture (s) and rapid proton capture (rp) processes, respectively. Reactions involving these nuclei contribute to the synthesis of the radioactive isotope ^{26}Al, whose 1.809 MeV γ-ray emission serves as a direct tracer of ongoing nucleosynthesis in the Galaxy. Understanding the detailed structure of these mirror systems is therefore crucial for refining astrophysical reaction rate calculations in stellar environments. This work uses the effective PSDPF interaction to theoretically investigate the excitation energies, spin-parity assignments, and transition probabilities of ^{25}Mg and ^{25}Al. We systematically compare the calculated results with available experimental data, demonstrating excellent agreement, and providing valuable constraints for modeling nucleosynthesis processes involving these nuclei.

DOI:10.5506/APhysPolBSupp.19.1-A6

1. Introduction

Study of *sd*-shell mirror nuclei provides valuable insights into the interplay between nuclear structure and fundamental symmetries, as well as processes relevant to stellar nucleosynthesis. In particular, the odd-mass mirror nuclei ^{25}Mg–^{25}Al are ideal candidates for studying the evolution of nuclear

* Presented at the XXXVIII Mazurian Lakes Conference on Physics, Piaski, Poland, August 31–September 6, 2025.

structure, offering detailed information on excitation energies, electromagnetic moments, and transition strengths. Situated near the line of stability, this mirror pair exhibits an intricate interplay between proton and neutron excitations that strongly influences the structure of their low-lying states. From a nuclear-structure perspective, the ^{25}Mg–^{25}Al system serves as an excellent testing ground for modern shell-model interactions. While ^{25}Mg is well-characterized experimentally, providing a reliable basis for mirror-symmetry comparisons, its partner ^{25}Al allows for detailed Coulomb energy difference analyses. Moreover, these nuclei are directly involved in several astrophysical reaction chains, linking nuclear structure studies with stellar nucleosynthesis [1]. The ^{22}Ne$(\alpha, n)^{25}$Mg reaction is recognized as the main neutron source in the slow neutron-capture (s) process occurring in massive stars and low-mass asymptotic giant branch (AGB) stars [2–4]. The produced ^{25}Mg nucleus plays a crucial role as a branching point: proton capture on ^{25}Mg leads to the formation of the long-lived radionuclide ^{26}Al [5], while neutron capture results in the stable isotope ^{26}Mg [6].

On the proton-rich side, the mirror nucleus ^{25}Al is important in the rapid proton capture (rp) process and in explosive stellar environments such as nova explosions and red giant stars [7]. The ^{22}Mg$(\alpha, p)^{25}$Al reaction [8] acts as a link between the Ne–Na and Mg–Al cycles, while the subsequent ^{25}Al$(p, \gamma)^{26}$Si reaction represents one of the key remaining uncertainties in modeling the abundance of radiogenic ^{26}Al ejected from classical novae [9]. Consequently, a consistent theoretical description of the spectroscopic properties of both ^{25}Mg and ^{25}Al is essential for improving the accuracy of astrophysical reaction-rate calculations and clarifying the structure of both bound and unbound states.

Shell-model calculations were performed employing the Nathan code [10] and PSDPF effective interaction [11]. The calculated excitation energies and the electromagnetic transition properties were systematically compared with available experimental data [12, 13] to assess the predictive power of our model.

2. Theoretical framework

In the shell-model framework, nuclear structure is described by an effective interaction acting within a defined valence space outside an inert core. The PSDPF effective interaction was developed by Bouhelal *et al.* [11] to provide a simultaneous description of both normal $0\hbar\omega$ and intruder $1\hbar\omega$ states in *sd*-shell nuclei. In this approach, the valence space is extended to the full *p*–*sd*–*pf* model space with a ^{4}He core, allowing one-nucleon cross-shell excitations between major shells. The PSDPF interaction was fitted in two steps. Positive-parity states were used to adjust the *sd*-shell part of the interaction, largely based on the USDB Hamiltonian [14] incorpo-

rated into PSDPF, by including known experimental positive-parity levels of all *sd*-shell nuclei. Negative-parity states were employed to adjust the remaining interaction parameters, including single-particle energies and cross-shell monopole and multipole terms. In the fitting procedure, only the first known negative-parity state for each spin was considered. Owing to the rapid growth of matrix dimensions, only nuclei at the beginning and the end of the *sd*-shell were included, namely $^{16-20}$O, $^{18-21}$F, $^{20-22}$Ne, ^{33,34}Si, ^{34,35}P, ^{35,36}S, $^{35-37}$Cl, $^{36-38}$Ar, ^{38,39}K, and ^{40}Ca. Nuclei in the middle of the *sd*-shell, from $Z = 10, A = 22$ to $Z = 14, A = 33$, could not be included in the fit and therefore provide an independent test of the predictive power of the interaction. This interaction has proven successful in reproducing the spectroscopic properties of nuclei in the *sd*-shell nuclei, as shown in [15, 16].

3. Results and discussion

In this section, we present a theoretical analysis of the nuclear structure properties in the ^{25}Mg–^{25}Al mirror nuclei, focusing on excitation energies and electromagnetic observables. As the PSDPF interaction is Coulomb-free and isospin-symmetric, identical excitation energies are obtained for the mirror nuclei.

3.1. Excitation energies

Experimentally, the energy spectrum of ^{25}Al has been extensively investigated up to $\sim$ 9 MeV through various reaction studies. While the low-lying levels of ^{25}Al are well established, the spin-parity assignments of many higher-lying states, particularly those above the proton separation energy (Sp = 2271.37 keV), remain uncertain. To complement these experimental efforts and achieve a comprehensive understanding of the excitation spectrum, a comparison with the well-known ^{25}Mg spectrum and with the shell-model calculations is crucial for clarifying the structure of both bound and unbound states in ^{25}Al. In this context, to evaluate the reliability of our shell-model predictions, we calculate the energy spectra, including both positive- and negative-parity states in the mirror pair, up to $\sim$ 9 MeV, and compare them with the available experimental data [12].

Figures 1 and 2 display the differences between the calculated and experimental excitation energies, for each parity sequence, defined as: $\Delta E = E_{\text{th}} - E_{\text{exp}}$. For both nuclei, the calculated excitation energies of the positive-parity states reproduce the experimental levels very well, with deviations generally within a few hundred keV. For the negative-parity states, the overall agreement with experiment is also satisfactory. Most states are well reproduced, with slightly larger deviations observed only for $3/2^-_1$ and $5/2^-_1$ levels. The ordering of the negative-parity states, particularly for higher spins, is consistent with the experimental data.

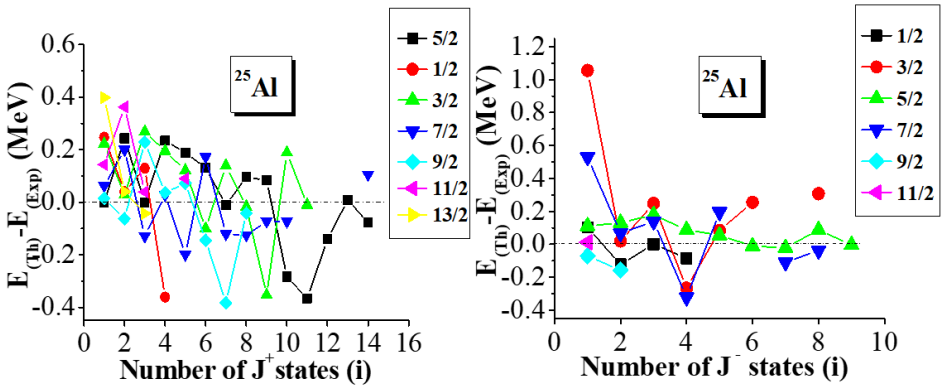

Fig. 1. Energy differences (in MeV) between experiment and theory for J^+ (left) and J^- (right) states in ^{25}Al.

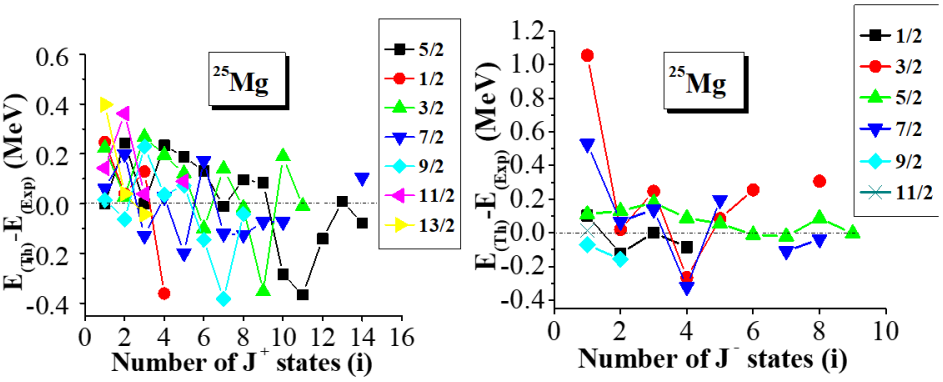

Fig. 2. Energy differences (in MeV) between experiment and theory for J^+ (left) and J^- (right) states in ^{25}Mg.

3.2. Electromagnetic transition properties

Electromagnetic transition properties provide stringent tests of shell-model predictions. In this section, the calculated B(E2) transition strengths, obtained using the effective charges for protons and neutrons taken from Ref. [17], as well as the magnetic dipole and electric quadrupole moments, are compared with the available experimental data [12, 13].

As shown in Fig. 3, the PSDPF interaction reproduces the experimental B(E2) values satisfactorily for both ^{25}Mg and ^{25}Al, with only minor underestimations for a few transitions.

For the magnetic dipole moments, the calculated values (^{25}Al; $\mu = 3.7399\ \mu_N$) and (^{25}Mg; $\mu = -0.85436\ \mu_N$) are in excellent agreement with experiment $\mu = 3.6455(12)\ \mu_N$ and $-0.85545(8)\ \mu_N$, respectively. This close correspondence confirms that the wave functions generated by the PSDPF interaction provide a realistic description of the spin and orbital contributions to the magnetic moments in the *sd*-shell region. Similarly, the calculated electric quadrupole moments (^{25}Al; $Q = 0.18$ b and ^{25}Mg; $Q = +0.202$ b) agree well with the measured values of 0.24(2) b and +0.201(3) b, respectively. The correct positive sign for both nuclei indicates a prolate intrinsic shape, demonstrating that the PSDPF interaction successfully captures the deformation and collective behavior of the $5/2^+_1$ ground states.

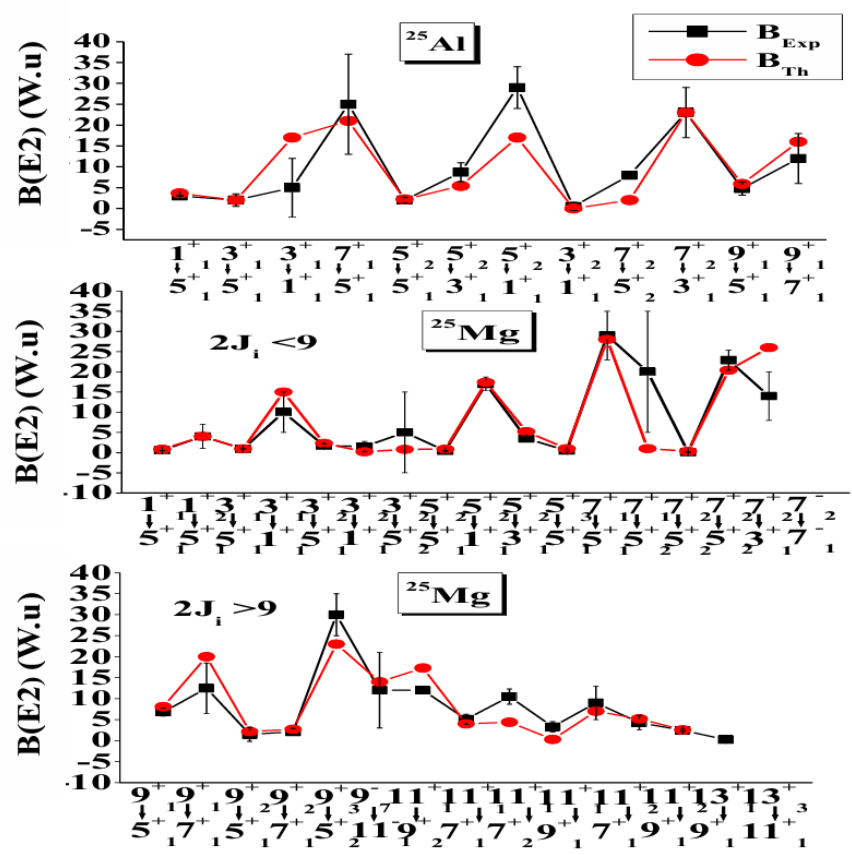

Fig. 3. Comparison of calculated and experimental $B(\mathrm{E2}; 2J_\mathrm{i} \rightarrow 2J_\mathrm{f})$ transition strengths for ^{25}Al and ^{25}Mg.

4. Summary

The PSDPF effective interaction provides a consistent and comprehensive shell-model description of the spectroscopic properties of the ^{25}Mg–^{25}Al mirror pair studied in this contribution. The calculated excitation energies, spin-parity assignments, and electromagnetic observables — including magnetic dipole, electric quadrupole moments, and electric transition strengths $B(\mathrm{E2})$ — show overall excellent agreement with available experimental data.

These results provide valuable nuclear-structure input for reaction-rate calculations involving the $^{25}\mathrm{Al}(p,\gamma)^{26}\mathrm{Si}$ and $^{25}\mathrm{Mg}(p,\gamma)^{26}\mathrm{Al}$ reactions, which are both essential for understanding the stellar production of the long-lived radioisotope ^{26}Al observed through its 1.809 MeV γ-ray emission.

REFERENCES

[1] T. Rauscher, F.-K. Thielemann, *At. Data Nucl. Data Tables* **75**, 1 (2000), specific information taken from pp. 23, 156–157, and 203–204.

[2] S. Ekström, *Front. Astron. Space Sci.* **8**, 617765 (2021).

[3] M. Pignatari *et al.*, *Astrophys. J.* **710**, 1557 (2010).

[4] R. Longland, C. Iliadis, A.I. Karakas, *Phys. Rev. C* **85**, 065809 (2012).

[5] F. Strieder *et al.*, *Phys. Lett. B* **707**, 60 (2012).

[6] P.L. Gay, D.L. Lambert, *Astrophys. J.* **533**, 260 (2000).

[7] D.C. Powell *et al.*, *Nucl. Phys. A* **660**, 349 (1999).

[8] A. Matic *et al.*, *Phys. Rev. C* **84**, 025801 (2011).

[9] L. Canete *et al.*, *Phys. Rev. C* **104**, L022802 (2021).

[10] E. Caurier, F. Nowacki, *Acta Phys. Pol. B* **30**, 705 (1999).

[11] M. Bouhelal *et al.*, *Nucl. Phys. A* **864**, 113 (2011).

[12] R.B. Firestone, *Nucl. Data Sheets* **110**, 1691 (2009).

[13] M.S. Basunia, A. Chakraborty, *Nucl. Data Sheets* **205**, 1 (2025).

[14] B.A. Brown, W.A. Richter, *Phys. Rev. C* **74**, 034315 (2006).

[15] K. Sieja, *Eur. Phys. J. A* **59**, 147 (2023).

[16] O. Le Noan, K. Sieja, *Phys. Rev. C* **111**, 064308 (2025).

[17] W.A. Richter, S. Mkhize, B.A. Brown, *Phys. Rev. C* **78**, 064302 (2008).